

Thermodynamics of Engineered Gold Binding Peptides: Establishing the Structure–Activity Relationships

Urartu Ozgur Safak Seker,^{†,‡,§,¶} Brandon Wilson,[†] John L. Kulp,[§] John S. Evans,[§] Candan Tamerler,^{†,⊥,#} and Mehmet Sarikaya*,^{†,‡,§,||}

[†]GEMSEC, Genetically Engineered Materials Science and Engineering Center, Department of Materials Science and Engineering, Roberts Hall, Box: 352120, Seattle, Washington 98195, United States

[‡]Department of Molecular Biology and Genetics, Istanbul Technical University, Maslak, Istanbul, Turkey

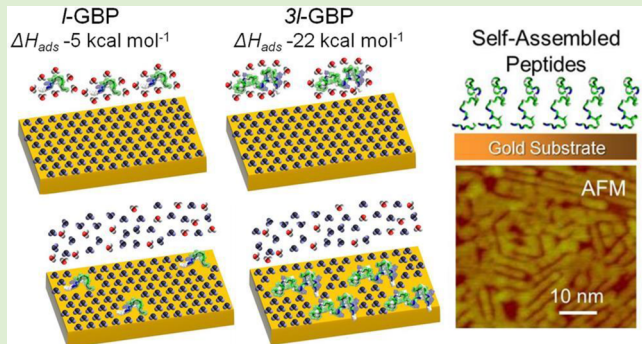
[§]Laboratory for Chemical Physics, New York University, 345 East 24th Street, New York, New York 10010, United States

^{||}Department of Chemical Engineering, University of Washington, Seattle, Washington 98195, United States

[#]Department of Mechanical Engineering and Bioengineering Research Center, The University of Kansas, Lawrence, Kansas 66045, United States

S Supporting Information

ABSTRACT: Adsorption behavior of a gold binding peptide was experimentally studied to achieve kinetics and thermodynamics parameters toward understanding of the binding of an engineered peptide onto a solid metal surface. The gold-binding peptide, GBP1, was originally selected using a cell surface display library and contains 14 amino acid residues. In this work, single- and three-repeats of GBP1 were used to assess the effects of two parameters: molecular architecture versus secondary structure on adsorption on to gold substrate. The adsorption measurements were carried out using surface plasmon resonance (SPR) spectroscopy at temperatures ranging from 10 to 55 °C. At all temperatures, two different regimes of peptide adsorption were observed, which, based on the model, correspond to two sets of thermodynamics values. The values of enthalpy, ΔH_{ads} , and entropy, ΔS_{ads} , in these two regimes were determined using the van't Hoff approach and Gibbs–Helmholtz relationship. In general, the values of enthalpy for both peptides are negative indicating GBP1 binding to gold is an exothermic phenomenon and that the binding of three repeat gold binding peptide (3l-GBP1) is almost 5 times tighter than that for the single repeat (1-GBP1). More intriguing result is that the entropy of adsorption for the 3l-GBP1 is negative (-43.4 ± 8.5 cal/(mol K)), while that for the 1-GBP1 is positive (10.90 ± 1.3 cal/(mol K)). Among a number of factors that synergistically contribute to the decrease of entropy, long-range ordered self-assembly of the 3l-GBP1 on gold surface is the most effective, probably through both peptide–solid and peptide–peptide intermolecular interactions. Additional adsorption experiments were conducted in the presence of 2,2,2-trifluoroethanol (TFE) to determine how the conformational structures of the biomolecules responded to the environmental perturbation. We found that the peptides differ in their conformational responses to the change in solution conditions; while 1-GBP does not fold in the presence of TFE, 3l-GBP1 adopted two types of secondary structure (β -strand, α -helix) and that peptide's binding to the solid is enhanced by the presence of low percentages of TFE solvent. Not only do these kinetics and thermodynamics results provide adsorption behavior and binding of genetically engineered peptides for inorganics (GEPI), but they could also provide considerable insights into fundamental understanding peptide molecular recognition and their selective specificity for the solids. Moreover, comprehensive work described herein suggests that multiple repeat forms of the solid binding peptides possess a conformational component that can be exploited to further tailor affinity and binding of a given sequence to a solid material followed by ordered assembly as a convenient tool in future practical applications.



INTRODUCTION

During the past decade, combinatorial peptide selection has been employed to generate sequence libraries toward a number of diverse inorganic solid surfaces, including metals,^{1–3} oxides,^{4,5} carbon materials,⁶ semiconductors^{7,8} and minerals.^{9,10} Phage¹¹ and cell surface display¹² have become the predominant approaches for material-specific peptide selection,

and solid binding peptides are rapidly becoming major molecular tools for biotechnological and nanotechnological applications.^{13–15} One of the first combinatorially selected

Received: December 24, 2013

Revised: May 30, 2014

Published: June 3, 2014

sequences was generated toward gold and is termed gold binding peptide, or GBP1.¹⁶ GBP1 has an extensive track record with regard to characterization and analysis that range from morphogenesis to immobilization of gold nanoparticles,¹⁷ directed immobilization of quantum dots,¹⁸ oriented immobilization of proteins,¹⁹ and development of biosensors by genetic fusion.^{14,20} Structural features of the single (l-GBP1) and triple (3l-GBP1) repeat versions, both in apo and Au (III)-bound forms, are primarily unfolded and labile in nature.²¹ The adsorption of 3l-GBP1 onto gold has been characterized using two major complementary techniques, namely, surface plasmon resonance spectroscopy (SPR) and quartz crystal microbalance (QCM)²² and, more recently, by atomic force microscopy (in particular, in terms of surface coverage and assembly).²³ In all these cases, the adsorption appears to proceed via a two-stage process which is not yet completely understood with regard to surface phenomena that may occur at the peptide–solid interface. Moreover, key energy and equilibrium terms that describe the adsorption of 3l-GBP1 and its shorter counterpart, l-GBP1, on gold surfaces are not known at this point.

To expand our observations beyond simple adsorption studies for the determination of kinetics parameters, which certainly provide essential knowledge-base for practical applications of these peptides,^{15,24,25} we now turn to the characterization methods that can quantify the thermodynamic terms and provide further fundamental insights into the two-stage adsorption process of the gold binding peptide observed on the gold substrate. Our overarching goal is, first, to understand the significance of fundamental phenomena in the binding of a peptide to a solid and, then, use this knowledge, in the future, in tailoring these peptide–solid soft interfaces for potential practical implementations, for example, their use as molecular linkers for targeted assembly, surface functionalization in biotechnology, and biominerization for nanoparticle formation. Previously, thermodynamics studies have been conducted to study the adsorption²⁶ of the proteins onto polymeric biomaterials and colloidal surfaces,^{27,28} chromatographic solid supports^{29,30} and on hydroxyapatite (HAP) using a general strategy that involves the use of calorimetric methods (e.g., DSC, differential scanning calorimetry, ITC, isothermal titration calorimetry).^{28,31} Also a surface-sensitive method, surface plasmon resonance (SPR) spectroscopy, has been frequently employed to determine the equilibrium thermodynamic parameters in the study of protein adsorption.^{32,33} In a benchmark study, equilibrium data generated from SPR experiments were found to be in good agreement with calorimetric data.³⁴ Thus, the SPR approach provides thermodynamics energy terms (ΔS , ΔG , ΔH), in addition to determining quantitative adsorption, desorption and equilibrium kinetics constants.

The characterization of naturally available solid binding proteins revealed that some of these proteins contain multiple repeats of the same peptide motifs. Some of the well-known samples are ice binding proteins,³⁵ lustrin, an aragonite binding protein found in mollusk shell,³⁶ collagens,³⁷ silaffins³⁸ and silicateins;³⁹ the last two catalyze silica synthesis in diatoms and sponge, respectively. These proteins contain multiple tandem repeats and they self-assemble into robust biomolecular architectures or become integral parts of the associated hard tissues. Using these evidence from nature in the previous studies, we explored the possibility of increasing the solid-binding affinity of the gold binding peptide, GBP1, as a function of the increase in the number of tandem repeats.⁴⁰ In

our previous work, it was noted that there is an initial increase in the binding affinity of GBP1 with the increasing number of tandem repeats (for example, 3–5 repeats) which then decreases eventually with higher number of repeats (e.g., 9 and 11).⁴¹ In this work, we chose 3-repeat as the example because of the significant increase in the binding affinity compared to that of the single repeat peptide⁴⁰ as well as the fact that this peptide self-assembles into ordered nanoarchitectures on Au(111).²³ Here, a more detailed thermodynamics analysis is carried out to understand the effect of the increasing repeats on the gold-binding capabilities by considering the binding enthalpy of one repeat versus three repeat of the peptides. In this report, specifically, the adsorption characteristics of the linear (as opposed to cyclic) forms of the MHGKTQATSGTIQS sequence designated as l-GBP1 and 3l-GBP1, were studied on thin solid gold film using SPR technique at temperatures between 25 and 55 °C to determine the effect of the repeat number on the behavior of the adsorption isotherms and, therefore, on binding equilibrium. In tandem with these studies, we investigated the secondary structure and the conformational stability of each form of l- and 3l-GBP1 in the presence of the structure-stabilizing solvent, namely, 2,2,2-trifluoroethanol (TFE).^{42,43} The TFE studies provide an indirect means of ascertaining the potential of each of the GBP1 biomolecules to undergo conformational reorganization in response to external perturbations. Our results suggest that the two-stage process of 3l-GBP1 adsorption on gold may involve polypeptide structural changes at some point during the overall surface processes making the peptide a better binder, while the single repeat peptide may lack this flexibility in the folding pattern and, therefore, lacks long-range ordered structures on the gold surface.²³

MATERIALS AND METHODS

Peptide Synthesis. l- and 3l-GBP-1 were synthesized using standard *Fmoc* solid phase peptide synthesis techniques and purified using C-18 reverse phase liquid chromatography (RPLC) to a level >95% (United Biochemical Research). Peptide solutions were prepared in phosphate buffer (1:3 mixtures of 10 mM KH₂PO₄, 10 mM K₂HPO₄, and 100 mM KCl). The pH of both buffers were adjusted to pH 7.5 using 0.1 M HCl and 0.1 M NaOH.

Circular Dichroism (CD) Experiments. Lyophilized synthetic l-GBP1 and 3l-GBP1 peptides were individually dissolved in distilled deionized water to create stock solutions. Each stock solution was then diluted to 30, 20, 15, 12, 9, and 6 μM for CD spectrometry measurements in 100 μM Tris-HCl (pH 7.5). On the basis of the studies of concentration variation, the optimal value for both peptides was chosen as 12 μM, and this concentration was utilized for further 2,2,2-trifluoroethanol (TFE, Acros Chemicals, 99.8%) titration studies (10, 20, 30, 50, 70, and 90 vol %). All CD spectra were obtained at 25 °C with an AVIV 60 CD Spectrometer, running 60DS software version 4.1t. The CD spectrometer was previously calibrated with d-10-camphorsulfonic acid. Wavelength scans were conducted from 185 to 260 nm with appropriate buffer and solvent background subtraction.^{2,17} For each spectrum, 3 scans were averaged using 1 nm bandwidth and a scanning rate of 0.5 nm/s. Mean residue ellipticity [$[\theta]_M$] is expressed in deg·cm²/dmol⁻¹.^{2,19}

Surface Plasmon Resonance (SPR) Spectroscopy. The SPR experiments were carried out using a custom-made instrument that consisted of a polychromatic light source (Ocean Optics LS1) that is connected to the detector via fiber optic cables.⁴⁴ To adjust the angle of incidence of the light, the collimator and detector sensors were placed on two mobile arms. The flow cell was manufactured from PTFE and placed on a goniometer; a Mylar gasket was used to prevent leaking between two channels. This instrument can detect changes at a level of 0.0001 refractive index units. The prism and glass slide were

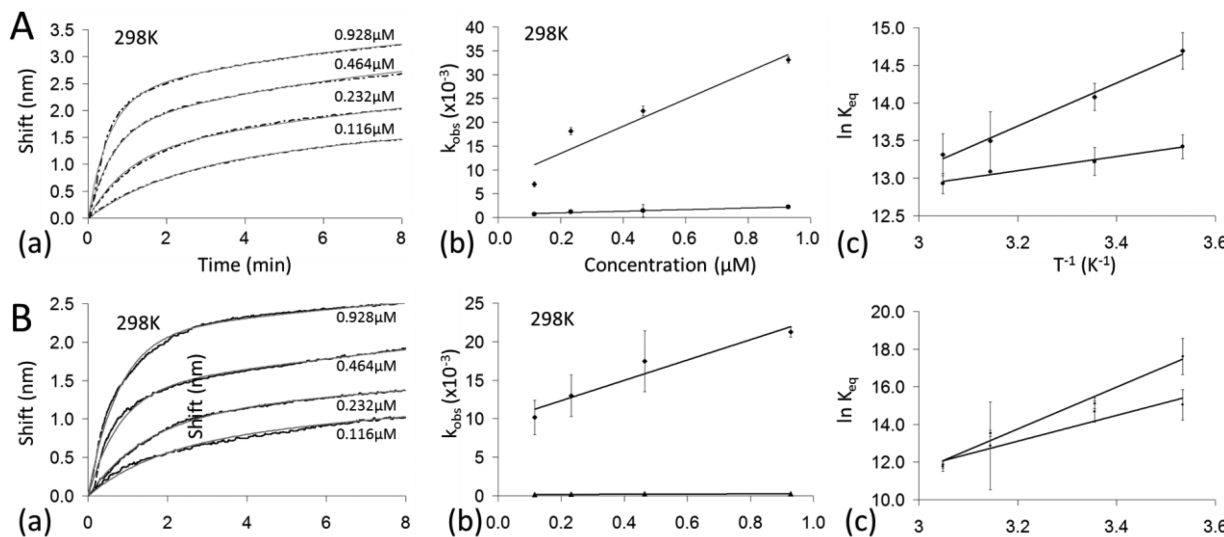


Figure 1. SPR Spectroscopic study of adsorption of peptides at various concentrations at room temperature for l-GBP1 (A) and for 3l-GBP1 (B). The plots in (a), (b), and (c) are the adsorption sensogram for peptides, observed adsorption rates as a function of time, and van't Hoff plots, respectively. The adsorption isotherms are shown in the Supporting Information.

both made of BK7 glass with a refractive index of 1.510, and the substrate was coupled with immersion oil having a refractive index of 1.510. The SPR slides were prepared by evaporating 2 nm Cr and 47 nm of Au onto the BK7 glass. The slides were rinsed with ethanol and water. To remove any possible organic contamination, SPR slides were treated with UV light/ozone for 5 min. For temperature stabilization, the samples were placed on a heat block that was equilibrated at the same temperature with SPR flow cell chamber. An embedded Peltier system was used to control temperature through the SPR flow channel. Adsorption data from SPR measurements were collected using Win Spectral software.

Both l- and 3l-GBP1 peptides were run at concentrations of 0.116, 0.23, 0.46, and 0.92 μM. Each of the experiments was carried out in triplicate. The data obtained were further used to construct adsorption isotherms for each temperature, using the analysis procedure described previously.³⁷

The determination of equilibrium constants at different temperatures enables us to calculate the entropy and enthalpy changes by using Gibbs–Helmholtz relationship, $\Delta G = -RT \ln K_{eq} = \Delta H - T\Delta S$. Simply, if one rewrites the Gibbs–Helmholtz relationship, which is now called van't Hoff equation,⁴⁵ as follows:

$$\ln K_{eq} = -\frac{\Delta H}{RT} + \frac{\Delta S}{R} \quad (1)$$

and then, plots $\ln K_{eq}$ versus $1/T$, one would then obtain entropy and enthalpy changes as the slope and the intersection of the line, respectively.

RESULTS AND DISCUSSION

In our previous studies, we reported the adsorption kinetics of a genetically engineered inorganic binding peptides that were determined via two different spectroscopic approaches, namely, quartz crystal microbalance (QCM) and surface plasmon resonance spectroscopy (SPR).²² The cited work was the first study for the quantitative evaluation of the affinity of one of the first combinatorially selected short, solid binding peptides using either of the two spectroscopic techniques. The SPR approach also allowed to monitor both the adsorption and the desorption behavior of the peptides in determining the thermodynamics fundamental parameters. The choice of gold as the solid substrate for adsorption offers an another ideal case as this relatively inert metal can be cleaned to obtain a pristine and

simple surface devoid of any oxides as compared to other metals, such as silver which oxidizes relatively fast, or oxide materials themselves, which readily adsorb molecular species, or semiconductors which have unknown, and not easily maintained, physicochemical surface characteristics; thus, gold would then potentially provide invaluable fundamental data for the understanding of the phenomena associated with peptide binding to a solid.

We first determined the certain kinetics parameters of l and 3l-GBP1 using the data obtained from SPR spectroscopy (Figure 1). Here, we calculated the equilibrium constants at different temperatures both for low and fast adsorption regimes (Table 1), and then used the van't Hoff relationship, given in eq

Table 1. Thermodynamic Parameters of Adsorption of GBP Determined by Equilibrium Analysis^a

parameters	l-GBP1	3l-GBP1
ΔH_1 (kcal/mol)	-5.09 ± 0.25	-22.1 ± 3.0
ΔH_2 (kcal/mol)	-1.84 ± 0.53	-13.4 ± 1.5
ΔS_1 (cal/mol·K)	$+10.90 \pm 1.30$	-43.4 ± 8.5
ΔS_2 (cal/mol·K)	$+19.60 \pm 2.20$	-16.6 ± 4.6
Surface Area (Å ²)	1738	4536
Volume (Å ³)	3493	10 010
Mass (Da)	1430.6	4291.8
pI (pH unit)	8.5	10
GRAVY	-0.7	-0.7
Charge (e)	+1	+3

^aThe amino acid sequence of the l-GBP is MHGKQATSGTIQS.

1, to calculate thermodynamics constants (Table 2). Similar to l-GBP1, the equilibrium adsorption coefficients for 3l-GBP1 decreases as a function of temperature. However, compared to l-GBP1, the peptide with tandem repeats, i.e., 3l-GBP1, has a larger change in equilibrium adsorption rate. Interestingly, the adsorption rate is decreased by a half for l-GBP1, whereas the corresponding rate for 3l-GBP1 increases more than 30 times as a function of temperature. The total change in K_{eq} is calculated as 4- and 300-fold for l-GBP1 and 3l-GBP1, respectively. We also note a large entropy change for 3l-

Table 2. Adsorption, Desorption, and Equilibrium Constants for l-GBP1 and 3l-GBP^a

T (K)	peptides	$k_a^1 \times 10^4$ (M ⁻¹ s ⁻¹)	$k_a^2 \times 10^3$ (M ⁻¹ s ⁻¹)	$k_d^1 \times 10^{-3}$ (s ⁻¹)	$k_d^2 \times 10^{-4}$ (s ⁻¹)	$K_{eq}^1 \times 10^6$ (M ⁻¹)	$K_{eq}^2 \times 10^5$ (M ⁻¹)
283	l-GBP1	2.16 ± 0.30	6.40 ± 0.64	7.18 ± 1.05	9.5 ± 0.60	3.07 ± 0.70	6.79 ± 1.10
	3l-GBP1	5.37 ± 0.80	3.64 ± 0.43	1.20 ± 1.54	10.7 ± 6.10	44.7 ± 11.0	34.2 ± 5.7
298	l-GBP1	1.36 ± 0.80	1.12 ± 0.20	8.88 ± 1.45	2.0 ± 0.00	1.56 ± 0.30	5.61 ± 1.05
	3l-GBP1	2.86 ± 0.16	1.66 ± 0.20	7.70 ± 1.83	6.50 ± 3.70	3.71 ± 1.22	32.7 ± 18.9
318	l-GBP1	1.43 ± 3.53	9.41 ± 4.69	14.0 ± 2.05	18.0 ± 2.20	1.07 ± 0.46	5.51 ± 3.55
	3l-GBP1	2.07 ± 0.44	2.47 ± 1.48	27.2 ± 1.10	47.3 ± 1.51	0.76 ± 0.30	5.23 ± 0.50
328	l-GBP1	1.65 ± 0.32	5.81 ± 0.80	21.0 ± 1.93	14.0 ± 0.00	0.80 ± 0.23	4.15 ± 0.57
	3l-GBP1	0.77 ± 0.14	0.75 ± 0.16	37.8 ± 0.64	56.7 ± 0.60	0.15 ± 0.04	1.32 ± 0.30

^aThe constants were calculated using the bimodal curve fitting; therefore, there are two different constants for each of the adsorption processes.

GBP1 upon binding, which indicates other processes have taken place besides simple adsorption process at the peptide–gold interface (Table 2). We propose that these changes are related to the differences in the chain length of the GBP1 molecule and, possibly, its folding pattern, as elaborated below.

Given the large, negative change in entropy associated with the binding of 3l-GBP1 onto Au surfaces, it is plausible to suggest that one of the events that occur during the two-stage polypeptide adsorption on to solid Au process is conformational rearrangement of the 42 AA sequences. Given that the solution structures of l- and 3l-GBP1 are both conformationally labile,²¹ we were curious to learn if either polypeptide exhibited tendencies to adopt specific conformations in response to changes in environment. Earlier, we established that M13 pIII phage tail sequences specific for Pt metal exhibited different structural responses to the structure-stabilizing solvent, 2,2,2-trifluoroethanol (TFE), and that these structural responses correlated with observed Pt–polypeptide affinities.⁴⁶ Thus, we utilized CD (circular dichroism) spectrometry and TFE solvent titrations to evaluate the response of the l- and 3l-GBP1 polypeptides to environmental perturbation (Figure 2).

As stated earlier, in the absence of TFE, both the l- and 3l-GBP1 molecules at pH 7.5 exist as an equilibrium mixture of random-coil and nonrandom coil conformations, as evidenced by the predominant $\pi-\pi^*$ transition-associated (−) ellipticity band centered at 195–198 nm (Figure 2). When TFE is introduced to l-GBP1, we note that the negative $\pi-\pi^*$ ellipticity band experiences a gradual red shift to 205 nm, a wavelength associated with beta turn conformation in equilibrium with random coil. Note that we do not observe the appearance of any other definitively ellipticity bands as a function of TFE content. However, when TFE is introduced to the 3l-GBP1 polypeptide, a different result is obtained (Figure 2). Here, at 10% (v/v) TFE content, we note the presence of three negative ellipticity bands centered at 200, 215, and 222 nm. The simultaneous presence of the 215 and 222 nm negative bands, which are characteristic of β -strand and α -helix, respectively, suggest that the 3l-GBP1 molecule exists in a nonrandom coil conformational equilibrium that possesses some degree of these two secondary structures. At 20% (v/v) TFE, a strong (+) ellipticity band appears at 192 nm, and (−) ellipticity bands at 208 and 222 nm, which increase in intensity as TFE content increases up to 90% (v/v). Thus, at TFE content of 20% (v/v) and higher, the conformational equilibrium of 3l-GBP1 polypeptide appears to shift yet again and the 42-AA sequence now adopts a predominantly α -helical structure in this solvent mixture.

From these results, we conclude the following: (a) Both the l- and 3l-GBP1 polypeptides can be further stabilized by the addition of TFE and can be induced to adopt nonrandom coil

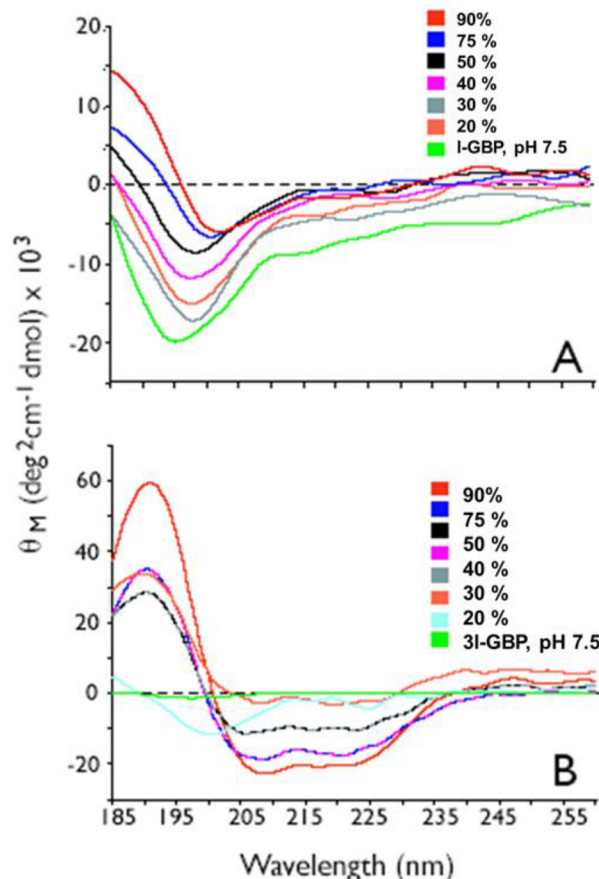


Figure 2. CD (circular dichroism) spectroscopy of (A) l-GBP1, and (B) 3l-GBP1, each in 100 μ M Tris-HCl buffer, pH 7.5, in the presence and absence of 2,2,2-trifluoroethanol (TFE). Note that in (B), there is an overlap between the 30%, 50% and 40%, 75% TFE ellipticity curves.

structures. (b) At TFE content >50% (v/v), each version of GBP1 adopts different secondary structures, indicating that, as a result of chain length differences, each GBP1 polypeptide responds differently to organic solvent perturbation. (c) At low TFE content (10–20% v/v), the longer 42-AA polypeptide exhibits two different, detectable secondary structures. We believe this feature is an indication of different folding capabilities that are inherent within 3l-GBP1.

Given the conformational effects that occur in the presence of TFE, we were curious to learn if this structure-stabilizing solvent also had an impact on GBP1 adsorption onto gold surface. To probe this, we chose the higher affinity 3l-GBP1 polypeptide and repeated our SPR binding experiments in the presence of TFE (Figure 3). Here, we note that the binding

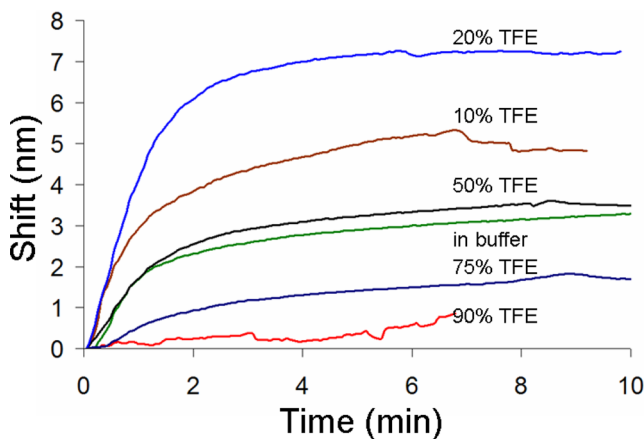


Figure 3. Binding affinity of 3l-GBP1 as a function of TFE (v/v, %) concentration. In the SPR sensograms for the 3l-GBP1 in varying TFE concentration, the shift represents the total change in the location of the SPR dip position. The magnitude of an SPR shift is related to a higher amount of peptide adsorbed on the surface of the gold.

isotherm in the presence of TFE is nonlinear, in contrast to what we observe under aqueous buffer conditions (Figure 3). Moreover, as shown in Figure 3, the binding affinity of 3l-GBP1 on gold surface changes in response to TFE content. We have calculated the initial adsorption rates (k_{obs}) of 3l-GBP at varying TFE concentrations. At TFE content of 10% and 20% (v/v), k_{obs} values are 4×10^{-2} and $5 \times 10^{-2} \text{ s}^{-1}$; we note that the binding affinity of 3l-GBP1 increases compared to aqueous buffer conditions where 3l-GBP has a k_{obs} value of 2.7×10^{-2} . At TFE content 50% (v/v), we observe a k_{obs} value, $2.8 \times 10^{-2} \text{ s}^{-1}$, which is similar to buffer conditions. A decreasing binding affinity, at 75% (v/v) TFE, 2×10^{-2} , and at 90% (v/v), $0.9 \times 10^{-2} \text{ s}^{-1}$ was observed so the binding affinity is abolished at these high TFE concentrations. Interestingly, the range of TFE content which induces higher affinity (10–20% v/v) correlates with the presence of different secondary structures (i.e., β -strand, α -helix) within the 3l-GBP1 polypeptide. These results indicate that TFE not only affects the conformation and stabilization of 3l-GBP1 in solution, but can modulate the affinity of this polypeptide for the gold surface, which further supports our conclusion that structural rearrangements are taking place within 3l-GBP1 during the adsorption process. Consequently, one can suggest that there is correlation of conformational instability (or adaptability) and binding capability.

In short, we successfully applied SPR to the thermodynamic analysis of the adsorption of a gold binding peptide, GBP-1, on a solid gold surface. We note a variety of general trends that are common to both the single and triple repeat forms. From the SPR data, we see two different regimes in the Langmuir isotherms which result in two sets of ΔH and ΔS values for l- and 3l-GBP1 as shown in Table 1. This two-stage growth behavior may be explained on the basis of the possible surface phenomena that accompany binding of the peptides to and their self-assembly on the gold substrate. Although the enthalpy and entropy changes are favorable for all steps of the binding process for each of the two polypeptides, it is the first step of the binding process that is more favorable than the assembly, the second step. These results indicate, therefore, that the binding process is thermodynamically significant to each peptide compared to the second step that involves surface organization. Although we do not yet definitively know the

details of the molecular event(s) that are involved in the first step of the binding process, from recent AFM observations it appears that as the peptides adsorb onto the Au surface they initially form small, isolated, flat islands.²³ The formation of these nanoislands, or nuclei, involves the binding of the molecules to the solid surface and their self-association, eventually establishing commensurate organization with the gold surface lattice to form long-range ordered biomolecular nanostructures, as evidenced by the presence of 6-fold symmetric domains in the AFM image (Figure 4). The

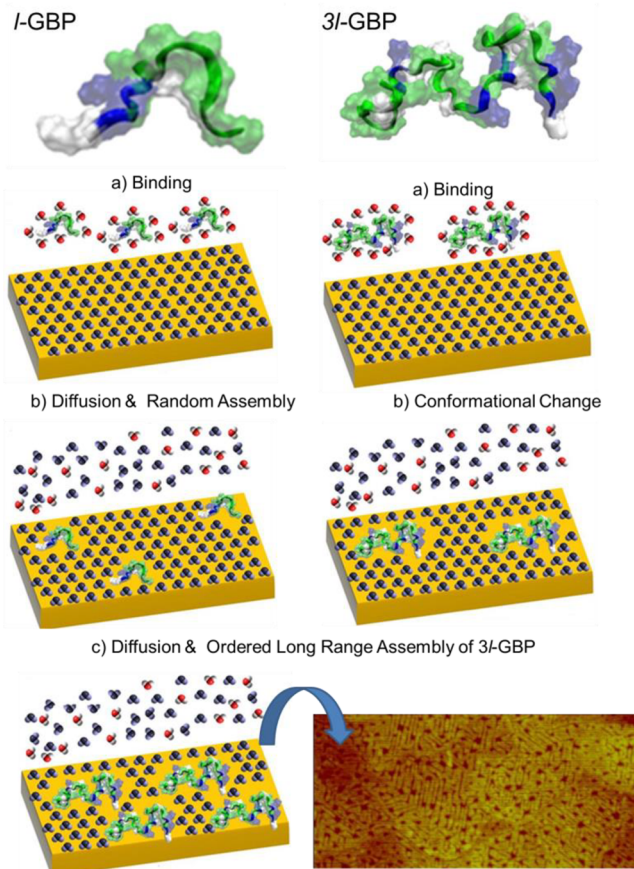


Figure 4. A hypothetical binding mechanism of the 1-GBP1 and 3l-GBP1 on a gold substrate through the change in the conformation of the GBP1 peptides. (a) Hydration layer is present where water molecules are adsorbed on the substrate, while 1-GBP1 and 3l-GBP1 start to react with the gold surface. (b) In 1-GBP1 case, the peptides are adsorbed on gold, loss of water off the surface dominates the adsorption process, and 3l-GBP1 peptides are in solution and start to react with the gold surface. While the 1-GBP1 molecules adsorbed and fixed on the surface, after adsorption on the gold surface, (c) 3l-GBP1 molecules undergo a significant conformational change followed by rearrangement and long-range ordered assembly. The AFM image of the long-range self-assembled 3l-GBP1 on the Au(111) surface showing 6-fold symmetric organized peptide domains.

significant insight that is emerging from the present study is that both of these two surface events would require displacement of surface water of hydration and, possibly, significant degree of internal reordering within the polypeptides themselves. Subsequently, these islands enlarge and branch out to form isolated dendritic, or fibrillar, nanostructures along specific crystallographic directions on the gold.²³ At the second step, as shown in Table 1, the surface events are favorable with

regard to entropy and enthalpy. The SPR data, and the AFM observations, reveal that the surface growth process of the adsorbed peptides initially occurs at a fast rate, and then decelerates after the initial of network formation has happened. Our interpretation, therefore, is that this second step involves internal polypeptide rearrangement processes for the biomolecules to assume surface folding pattern as to reduce the interface energy, which is then led by the additional branching and growth of the self-assembling peptides in ordered nanostructures on the crystallographically well-defined gold surface to form a highly symmetric network which eventually grows to cover the entire surface as a monomolecular-thick peptide film.^{23,47}

In short, both 1- and 3l-GBP1 requires two stages, with the enthalpy and entropy terms corresponding to the first stage being lower than those of the second stage. However, what distinguishes the single from the triple repeat form is the magnitude of the enthalpic and entropic terms (Table 1). Specifically, larger entropy and enthalpy changes are noted for 3l-GBP1 over 1-GBP1 in both stages of the binding process. We attribute these thermodynamic differences not only to variations in chain length, but to other molecular factors such as the extent of self-assembly on the Au surface and the inherent differences in associated conformational stability. It is likely that the triple repeat may require greater rearrangement, structural changes, and surface water displacement during adsorption onto the gold surface compared to the shorter single repeat peptide. To some extent, this is supported by our CD studies, which note that (a) the triple repeat GBP1 molecule can adopt two different secondary structures in response to external perturbation reagents (10% TFE)), and (b) the biomolecules of 1- and 3l-GBP1 do not adopt the same conformations in response to TFE (Figure 2). We envision that the adsorption of 1- and 3l-GBP1 molecules at solid–gold interfaces involves common key events. The adsorption process for both molecules most likely involves polypeptide interaction with adsorbed water molecules on the Au surfaces, desorption of the adsorbed water molecules in exchange with the corresponding peptide molecule, and a subsequent loss of solvent ordering on the surface. However, for 3l-GBP1, the presence of a large, positive entropy change suggests that another important step must take place as well. The basis of entropy change may originate from the stability of molecules in solution versus that on the surface, conformational changes of the molecules on the surface, and the final long-range ordered supramolecular assembly of the 3l-GBP1. As shown by our CD/TFE studies, conformational rearrangement can occur within the 3l-GBP1 molecule, and we believe that this process also takes place at the gold interface as well.

CONCLUSION

We conclude that conformational change controls the binding of 3l-GBP1 on gold interfaces to a greater extent than that it does for 1-GBP1. The predicted structures of 1-GBP1 and 3l-GBP1 and the suggested binding mechanisms are schematically presented in Figure 4. Here, in the case of 1-GBP1, desorption of the adsorbed water molecules from the surface dominates in the overall entropy term, which is a positive and is a characteristic of hydrophobic interactions. However, in the case of 3l-GBP1, both of the phenomena, i.e., the water desorption and peptide conformational changes, are the dominating factors in the overall process of peptide–solid interaction. Our experimental findings support the hypothesis

that water molecules immediately near the surface are directly involved in, and can mediate, the binding of the peptides onto the solid surface.⁴⁸ A recent computational study demonstrated that multiple repeats of GBP1 have high affinity to gold surface. It was concluded that if the gold binding peptides would have a high degree of conformational flexibility, and similar to those we see in this study in 3-repeats, the binding would be stronger.⁴⁹ Also, in a separate study the role of water molecules are found to be important for the surface recognition of the gold binding peptides; here the side chain and hydration layer of the peptides cooperate in way that the gold binding peptide achieves better binding.⁵⁰ The need for the displacement of the water molecules is noted as a major event during the adsorption process, which is also the case in our work.⁴⁹ Our results may shed more light into explaining such processes in terms of the displacement of water molecules from the surface that can be achieved by the high structural flexibility of the peptide molecules that manifest themselves in the conformational change during the binding. The structural studies carried out in the present work indicate that the conformational flexibility of the 3l-GBP1 is higher so that one would expect a stronger binding on the gold surface leading to the value of the enthalpy of binding for 3l-GBP being ~4 times higher than that for 1-GBP.

In the formation of biological hard tissues that have intricate hierarchical structures from the nanometer to macro scales, it is known that proteins and peptides play the major role of mineral synthesis, crystal formation, growth, and their morphogenesis.^{51–53} Proteins associated in natural biomineral formation are known to contain domains of acidic residues and are frequently encountered to be in the form of repeating units along the AA sequence.^{36,38,39} Biomineralizing proteins have probably evolved to incorporate repeats of specific peptide motifs which, when adsorbed and folded onto the solid, form a stereochemical structural interaction with the crystal surface of the biomineral.^{54–57} It follows from this, therefore, that the natural proteins interacting with mineral surfaces have repeating units, instead of single motifs, for thermodynamically favorable interactions with minerals and their specific crystallographic surfaces. Our results confirm these hypotheses where repeating polypeptides, such as 3l-GBP1, has an increased binding enthalpy compared to the single repeat 1-GBP1. In addition to providing invaluable thermodynamics parameters described herein, the new insights gained from the present work may be further utilized in the controlled biomineralization of the inorganic solid materials toward forming specific crystal shapes, morphologies, and organizations with tailored functionalities prescribed by the sequence-related conformational behavior of solid binding peptides toward a wide range of bionanotechnological and nanomedical applications through controlled biomineralization.

In summary, significant insight can be gained by quantitatively interrogating the binding affinity of the native, first generation biocombinatorially selected peptides as well as second generation, postselection engineered repeating peptides. As detailed herein, this is accomplished by studying thermodynamics as well as kinetics of specific biomolecular binding onto the associated solid. As demonstrated with one-repeat versus 3-repeat gold binding peptides, quantitative adsorption studied by SPR spectroscopy on the gold surface provides detailed information concerning the mode of binding, the kinetics, and energetic contributions leading to peptide self-

assembly on the crystallographically well-defined surface (e.g., Au(111)).

The main conclusion drawn from the proposed mechanism is that the use of multiple sequence repeats for higher affinity material binding invariably introduces a conformational term that can influence the rate and affinity of that polypeptide for a given, particular solid surface. The phenomena encountered between GBP1/gold surfaces may also be true for the majority of genetically derived, material-selective sequences. If so, then careful selection of the inherent and inducible conformation(s) of a particular polypeptide sequence could affect the resulting adsorption rate and affinity and, thus, allow “designing” the resulting bio/nano soft interface tailored for a variety of technological applications in which interface structures and functions are key in enabling a wide range of practical implementations.^{1–4,6–9,14,15,58–61}

ASSOCIATED CONTENT

Supporting Information

Details of the thermodynamic analysis and all of the data collected for the thermodynamic analysis, details of the adsorption model and equations, adsorption equilibrium constants for each temperature. This material is available free of charge via the Internet at <http://pubs.acs.org>.

AUTHOR INFORMATION

Corresponding Author

*Address: Materials Science and Engineering, University of Washington, Roberts Hall, Box: 352120; Seattle, WA 98195, USA. Phone: (206) 543-0724. Fax: (206) 543-6381. E-mail: sarikaya@u.washington.edu.

Present Addresses

[⊗]MIT Synthetic Biology Center and Research Laboratory of Electronics, Cambridge, MA,

[#]Department of Mechanical Engineering, The University of Kansas, Lawrence, KS 66045, USA,

Author Contributions

The manuscript was written through contributions of all authors. All authors have given approval to the final version of the manuscript.

Notes

The authors declare no competing financial interest.

ACKNOWLEDGMENTS

This study was supported by National Science Foundation (DMR-0520567) through GEMSEC, the Genetically Engineered Materials Science & Engineering Center at UW (M.S.) and, TUBITAK/NSF-IRES Joint Project(107T250) and Turkish State Planning Organization (DPT) through The Advanced Technologies Program at Istanbul Technical University (C.T.). Portions of this work represent contribution number 39 from the Laboratory for Chemical Physics, NYU (J.S.E.). We thank Christopher R. So for discussion and input. We thank Dr. E. Emre Oren for his help with drawings.

REFERENCES

- (1) Sarikaya, M.; Tamerler, C.; Jen, A. K. Y.; Schulten, K.; Baneyx, F. Molecular biomimetics: nanotechnology through biology. *Nat. Mater.* **2003**, *2* (9), 577–585.
- (2) Kim, J.; Rheem, Y.; Yoo, B.; Chong, Y.; Bozhilov, K. N.; Kim, D.; Sadowsky, M. J.; Hur, H. G.; Myung, N. V. Peptide-mediated shape-and size-tunable synthesis of gold nanostructures. *Acta Biomater.* **2010**, *6* (7), 2681–2689.
- (3) Naik, R. R.; Stringer, S. J.; Agarwal, G.; Jones, S. E.; Stone, M. O. Biomimetic synthesis and patterning of silver nanoparticles. *Nat. Mater.* **2002**, *1* (3), 169–172.
- (4) Naik, R. R.; Brott, L. L.; Clarson, S. J.; Stone, M. O. Silica-precipitating peptides isolated from a combinatorial phage display peptide library. *J. Nanosci Nanotechnol.* **2002**, *2* (1), 95–100.
- (5) Togashi, T.; Yokoo, N.; Umetsu, M.; Ohara, S.; Naka, T.; Takami, S.; Abe, H.; Kumagai, I.; Adschari, T. Material-binding peptide application—ZnO crystal structure control by means of a ZnO-binding peptide. *J. Biosci. Bioeng.* **2011**, *111* (2), 140–145.
- (6) Wang, S.; Humphreys, E. S.; Chung, S. Y.; Delduco, D. F.; Lustig, S. R.; Wang, H.; Parker, K. N.; Rizzo, N. W.; Subramoney, S.; Chiang, Y. M.; Jagota, A. Peptides with selective affinity for carbon nanotubes. *Nat. Mater.* **2003**, *2* (3), 196–200.
- (7) Lee, S. W.; Mao, C.; Flynn, C. E.; Belcher, A. M. Ordering of quantum dots using genetically engineered viruses. *Science* **2002**, *296* (5569), 892–895.
- (8) Mao, C.; Flynn, C. E.; Hayhurst, A.; Sweeney, R.; Qi, J.; Georgiou, G.; Iverson, B.; Belcher, A. M. Viral assembly of oriented quantum dot nanowires. *Proc. Natl. Acad. Sci. U.S.A.* **2003**, *100* (12), 6946–6951.
- (9) Chiu, D.; Zhou, W.; Kitayaporn, S.; Schwartz, D. T.; Murali-Krishna, K.; Kavanagh, T. J.; Baneyx, F. Biominerization and size control of stable calcium phosphate core-protein shell nanoparticles: potential for vaccine applications. *Bioconjugate Chem.* **2012**, *23* (3), 610–611.
- (10) Curtis, S. B.; Hewitt, J.; MacGillivray, R. T. A.; Dunbar, W. S. Biomining with bacteriophage: selectivity of displayed peptides for naturally occurring sphalerite and chalcopyrite. *Biotechnol. Bioeng.* **2009**, *102* (2), 644–650.
- (11) Smith, G. P. Filamentous fusion phage—novel expression vectors that display cloned antigens on the virion surface. *Science* **1985**, *228* (4705), 1315–1317.
- (12) Wittrup, K. D. Protein engineering by cell-surface display. *Curr. Opin. Biotechnol.* **2001**, *12* (4), 395–399.
- (13) Seker, U. O. S.; Ozel, T.; Demir, H. V. Peptide-mediated constructs of quantum dot nanocomposites for enzymatic control of nonradiative energy transfer. *Nano Lett.* **2011**, *11* (4), 1530–1539.
- (14) Krauland, E. M.; Peele, B. R.; Wittrup, K. D.; Belcher, A. M. Peptide tags for enhanced cellular and protein adhesion to single-crystal line sapphire. *Biotechnol. Bioeng.* **2007**, *97* (5), 1009–1020.
- (15) Demir, H. V.; Seker, U. O. S.; Zengin, G.; Mutlugun, E.; Sari, E.; Tamerler, C.; Sarikaya, M. Spatially Selective assembly of quantum dot light emitters in an LED using engineered peptides. *ACS Nano* **2011**, *5* (4), 2735–2741.
- (16) Brown, S. Metal-recognition by repeating polypeptides. *Nat. Biotechnol.* **1997**, *15* (3), 269–272.
- (17) Nochomovitz, R.; Amit, M.; Matmor, M.; Ashkenasy, N. Bioassisted multi-nanoparticle patterning using single-layer peptide templates. *Nanotechnology* **2010**, *21* (14), No. 145305.
- (18) Yokoo, N.; Togashi, T.; Umetsu, M.; Tsumoto, K.; Hattori, T.; Nakanishi, T.; Ohara, S.; Takami, S.; Naka, T.; Abe, H.; Kumagai, I.; Adschari, T. Direct and selective immobilization of proteins by means of an inorganic material-binding peptide: discussion on functionalization in the elongation to material-binding peptide. *J. Phys. Chem. B* **2010**, *114* (1), 480–486.
- (19) Hattori, T.; Umetsu, M.; Nakanishi, T.; Sawai, S.; Kikuchi, S.; Asano, R.; Kumagai, I. A high-affinity gold-binding camel antibody: antibody engineering for one-pot functionalization of gold nanoparticles as biointerface molecules. *Bioconjugate Chem.* **2012**, *23* (9), 1934–1944.
- (20) Park, T. J.; Lee, S. Y.; Lee, S. J.; Park, J. P.; Yang, K. S.; Lee, K. B.; Ko, S.; Park, J. B.; Kim, T.; Kim, S. K.; Shin, Y. B.; Chung, B. H.; Ku, S. J.; Kim, D. H.; Choi, I. S. Protein nanopatterns and biosensors using gold binding polypeptide as a fusion partner. *Anal. Chem.* **2006**, *78* (20), 7197–7205.

- (21) Kulp Iii, J. L.; Sarikaya, M.; Spencer Evans, J. Molecular characterization of a prokaryotic polypeptide sequence that catalyzes Au crystal formation. *J. Mater. Chem.* **2004**, *14* (14), 2325–2332.
- (22) Tamerler, C.; Oren, E. E.; Duman, M.; Venkatasubramanian, E.; Sarikaya, M. Adsorption kinetics of an engineered gold binding peptide by surface plasmon resonance spectroscopy and a quartz crystal microbalance. *Langmuir* **2006**, *22* (18), 7712–7718.
- (23) So, C. R.; Tamerler, C.; Sarikaya, M. Adsorption, diffusion, and self-assembly of an engineered gold-binding peptide on Au(111) investigated by atomic force microscopy. *Angew. Chem., Int. Ed.* **2009**, *48* (28), 5174–5177.
- (24) Lee, Y. J.; Yi, H.; Kim, W. J.; Kang, K.; Yun, D. S.; Strano, M. S.; Ceder, G.; Belcher, A. M. Fabricating genetically engineered high-power lithium-ion batteries using multiple virus genes. *Science* **2009**, *324* (5930), 1051–1055.
- (25) Cui, Y.; Kim, S. N.; Jones, S. E.; Wissler, L. L.; Naik, R. R.; McAlpine, M. C. Chemical functionalization of graphene enabled by phage displayed peptides. *Nano Lett.* **2010**, *10*, 4559–4565.
- (26) Tang, Z.; Palafox-Hernandez, J. P.; Law, W. C.; Z, E. H.; Swihart, M. T.; Prasad, P. N.; Knecht, M. R.; Walsh, T. R. Biomolecular recognition principles for bionanocombinatorics: an integrated approach to elucidate enthalpic and entropic factors. *ACS Nano* **2013**, *7* (11), 9632–9646.
- (27) Seker, U. O.; Mutlugu, E.; Hernandez-Martinez, P. L.; Sharma, V. K.; Lesnyak, V.; Gaponik, N.; Eychmuller, A.; Demir, H. V. Bionanohybrids of quantum dots and photoproteins facilitating strong nonradiative energy transfer. *Nanoscale* **2013**, *5* (15), 7034–7040.
- (28) Kandori, K.; Murata, K.; Ishikawa, T. Microcalorimetric study of protein adsorption onto calcium hydroxyapatites. *Langmuir* **2007**, *23* (4), 2064–2070.
- (29) Lin, F. Y.; Chen, W. Y.; Hearn, M. T. W. Microcalorimetric studies on the interaction mechanism between proteins and hydrophobic solid surfaces in hydrophobic interaction chromatography: Effects of salts, hydrophobicity of the sorbent, and structure of the protein. *Anal. Chem.* **2001**, *73* (16), 3875–3883.
- (30) Vailaya, A.; Horvath, C. Enthalpy entropy compensation in hydrophobic interaction chromatography. *J. Phys. Chem.* **1996**, *100* (6), 2447–2455.
- (31) Goobes, R.; Goobes, G.; Campbell, C. T.; Stayton, P. S. Thermodynamics of statherin adsorption onto hydroxyapatite. *Biochemistry* **2006**, *45* (17), 5576–5586.
- (32) Day, Y. S. N.; Baird, C. L.; Rich, R. L.; Myszka, D. G. Direct comparison of binding equilibrium, thermodynamic, and rate constants determined by surface- and solution-based biophysical methods. *Protein Sci.* **2002**, *11* (5), 1017–1025.
- (33) Cannon, M. J.; Myszka, D. G.; Bagnato, J. D.; Alpers, D. H.; West, F. G.; Grissom, C. B. Equilibrium and kinetic analyses of the interactions between vitamin B-12 binding proteins and cobalamins by surface plasmon resonance. *Anal. Biochem.* **2002**, *305* (1), 1–9.
- (34) Navratilova, I.; Papalia, G. A.; Rich, R. L.; Bedinger, D.; Brophy, S.; Condon, B.; Deng, T.; Emerick, A. W.; Guan, H. W.; Hayden, T.; Heutmakers, T.; Hoorebeke, B.; McCroskey, M. C.; Murphy, M. M.; Nakagawa, T.; Parmeggiani, F.; Qin, X. C.; Rebe, S.; Tomasevic, N.; Tsang, T.; Waddell, M. B.; Zhang, F. F.; Leavitt, S.; Myszka, D. G. Thermodynamic benchmark study using Biacore technology. *Anal. Biochem.* **2007**, *364* (1), 67–77.
- (35) Sicheri, F.; Yang, D. S. C. Ice-binding structure and mechanism of an antifreeze protein from winter flounder. *Nature* **1995**, *375* (6530), 427–431.
- (36) Shen, X. Y.; Belcher, A. M.; Hansma, P. K.; Stucky, G. D.; Morse, D. E. Molecular cloning and characterization of lustrin A, a matrix protein from shell and pearl nacre of *Haliotis rufescens*. *J. Biol. Chem.* **1997**, *272* (51), 32472–32481.
- (37) Rich, A.; Crick, F. H. C. Structure of Collagen. *Nature* **1955**, *176* (4489), 915–916.
- (38) Kroger, N.; Deutzmann, R.; Sumper, M. Silica-precipitating peptides from diatoms—The chemical structure of silaffin-1A from *Cylindrotheca fusiformis*. *J. Biol. Chem.* **2001**, *276* (28), 26066–26070.
- (39) Shimizu, K.; Cha, J.; Stucky, G. D.; Morse, D. E. Silicatein alpha: Cathepsin L-like protein in sponge biosilica. *Proc. Natl. Acad. Sci. U.S.A.* **1998**, *95* (11), 6234–6238.
- (40) Seker, U. O. S.; Wilson, B.; Sahin, D.; Tamerler, C.; Sarikaya, M. Quantitative affinity of genetically engineered repeating polypeptides to inorganic surfaces. *Biomacromolecules* **2009**, *10* (2), 250–257.
- (41) Kacar, T.; Zin, M. T.; So, C.; Wilson, B.; Ma, H.; Gul-Karaguler, N.; Jen, A. K. Y.; Sarikaya, M.; Tamerler, C. Directed self-immobilization of alkaline phosphatase on micro-patterned substrates via genetically fused metal-binding peptide. *Biotechnol. Bioeng.* **2009**, *103* (4), 696–705.
- (42) Sonnichsen, F. D.; Van Eyk, J. E.; Hodges, R. S.; Sykes, B. D. Effect of trifluoroethanol on protein secondary structure: an NMR and CD study using a synthetic actin peptide. *Biochemistry* **1992**, *31* (37), 8790–8798.
- (43) Buck, M. Trifluoroethanol and colleagues: cosolvents come of age. Recent studies with peptides and proteins. *Q. Rev. Biophys.* **1998**, *31* (3), 297–355.
- (44) Dostalek, J.; Homola, J.; Miler, M. Rich information format surface plasmon resonance biosensor based on array of diffraction gratings. *Sens. Actuators, B* **2005**, *107* (1), 154–161.
- (45) Atkins, P. W. *Physical Chemistry*; Oxford University Press: Oxford, 1978.
- (46) Seker, U. O. S.; Wilson, B.; Dincer, S.; Kim, I. W.; Oren, E. E.; Evans, J. S.; Tamerler, C.; Sarikaya, M. Adsorption behavior of linear and cyclic genetically engineered platinum binding peptides. *Langmuir* **2007**, *23* (15), 7895–7900.
- (47) So, C. R.; Kulp, J. L.; Oren, E. E.; Zareie, H.; Tamerler, C.; Evans, J. S.; Sarikaya, M. Molecular recognition and supramolecular self-assembly of a genetically engineered gold binding peptide on Au{111}. *ACS Nano* **2009**, *3* (6), 1525–1531.
- (48) Ghiringhelli, L. M.; Hess, B.; van der Vegt, N. F. A.; Delle Site, L. Competing adsorption between hydrated peptides and water onto metal surfaces: From electronic to conformational properties. *J. Am. Chem. Soc.* **2008**, *130* (40), 13460–13464.
- (49) Verde, A. V.; Acres, J. M.; Maranas, J. K. Investigating the specificity of peptide adsorption on gold using molecular dynamics simulations. *Biomacromolecules* **2009**, *10* (8), 2118–2128.
- (50) Calzolari, A.; Cicero, G.; Cavazzoni, C.; Di Felice, R.; Catellani, A.; Corni, S. Hydroxyl-rich beta-sheet adhesion to the gold surface in water by first-principle simulations. *J. Am. Chem. Soc.* **2010**, *132* (13), 4790–4795.
- (51) Suzuki, M.; Dauphin, Y.; Addadi, L.; Weiner, S. Atomic order of aragonite crystals formed by mollusks. *CrystEngComm* **2011**, *13* (22), 6780–6786.
- (52) Politi, Y.; Metzler, R. A.; Abrecht, M.; Gilbert, B.; Wilt, F. H.; Sagi, I.; Addadi, L.; Weiner, S.; Gilbert, P. Transformation mechanism of amorphous calcium carbonate into calcite in the sea urchin larval spicule. *Proc. Natl. Acad. Sci. U.S.A.* **2008**, *105* (45), 17362–17366.
- (53) Cölfen, H. *Mesocrystals and Nonclassical Crystallization*; Wiley: Hoboken, NJ, 2008.
- (54) Green, D.; Walsh, D.; Mann, S.; Oreffo, R. O. C. The potential of biomimesis in bone tissue engineering: Lessons from the design and synthesis of invertebrate skeletons. *Bone* **2002**, *30* (6), 810–815.
- (55) Shiba, K.; Honma, T.; Minamisawa, T.; Nishiguchi, K.; Noda, T. Distinct macroscopic structures developed from solutions of chemical compounds and periodic proteins. *EMBO Rep.* **2003**, *4* (2), 148–153.
- (56) Shiba, K.; Minamisawa, T. A synthesis approach to understanding repeated peptides conserved in mineralization proteins. *Biomacromolecules* **2007**, *8* (9), 2659–2664.
- (57) Weiner, S.; Addadi, L. Crystallization Pathways in Biominerilization. In *Annual Review of Materials Research*; Clarke, D. R., Fratzl, P., Eds.; Annual Reviews: Palo Alto, CA, 2011; Vol. 41, pp 21–40.
- (58) Wang, G. C.; Cao, R. Y.; Chen, R.; Mo, L. J.; Han, J. F.; Wang, X. Y.; Xu, X. R.; Jiang, T.; Deng, Y. Q.; Lyu, K.; Zhu, S. Y.; Qin, E. D.; Tang, R. K.; Qin, C. F. Rational design of thermostable vaccines by engineered peptide-induced virus self-biominerilization under physiological conditions. *Proc. Natl. Acad. Sci. U.S.A.* **2013**, *110* (19), 7619–7624.

- (59) Galloway, J. M.; Bramble, J. P.; Staniland, S. S. Biomimetic synthesis of materials for technology. *Chem.—Eur. J.* **2013**, *19* (27), 8710–8725.
- (60) Manikas, A. C.; Causa, F.; Della Moglie, R.; Netti, P. A. Tuning gold nanoparticles interfaces by specific peptide interaction for surface enhanced raman spectroscopy (SERS) and separation applications. *ACS Appl. Mater. Interfaces* **2013**, *5* (16), 7915–7922.
- (61) Togashi, T.; Yokoo, N.; Umetsu, M.; Ohara, S.; Naka, T.; Takami, S.; Abe, H.; Kumagai, I.; Adschiri, T. Material-binding peptide application-ZnO crystal structure control by means of a ZnO-binding peptide. *J. Biosci. Bioeng.* **2011**, *111*, 140–145.